Analyst

Check for updates

ROYAL SOCIETY OF CHEMISTRY

Electrochemical Hg²⁺ detection at tannic acid-gold nanoparticle modified electrodes by square wave voltammetry†

Alex L. Suherman, [a] Sabine Kuss,[a] Eden E. L. Tanner, ‡[a] Neil P. Young[b] and Richard G. Compton *[a]

We report the electrochemical sensing of Hg²⁺ based on tannic acid capped gold nanoparticle (AuNP@TA) complexes. At optimal conditions using square wave voltammetry, the presented analytical method exhibits a "measurable lower limit" of 100.0 fM. This limit is considerably below the permissible level of 30.0 nM for inorganic mercury in drinking water, specified by the World Health Organization (WHO). The effect of potentially interfering ions, such as Zn²⁺ and Al³⁺, was studied and results indicate an excellent selectivity for Hg²⁺. The transfer of the proposed strategy onto AuNP@TA modified screen-printed electrodes demonstrates its applicability to routine monitoring of Hg²⁺ in tap water.

Introduction

The World Health Organisation (WHO) has declared mercury as one of the most toxic heavy metals to human health.[1] Inorganic mercury (Hg²⁺) accumulates in the vital tissues and organs, interfering with proteins and enzymes,[2] which can result in cellular dysfunctions and health issues, such as learning and memory impairments, as well as Alzheimer's disease.[3–5] In addition, individuals with congenital mercury toxicity are especially vulnerable to environmental mercury contaminations and may show severe mental retardation[6] and neurological abnormalities,[7] as well as profound immunological and embryonic toxicological effects.[8] Therefore, the exposure to inorganic Hg²⁺ by the consumption of contaminated drinking water has become a global concern and a maximum permissible level of Hg²⁺ in drinking water of 6.0 µg L⁻¹ was declared by the WHO, which corresponds to an approximate concentration of 30.0 nM.[1]

The above-mentioned risks associated with inorganic Hg²⁺ in drinking water require sensitive and selective detection and monitoring strategies to assure public health. To date, various analytical methods have been developed for the detection of trace and/or ultra-trace levels of Hg²⁺, such as gas chromatography-inductively coupled plasma analysis (GC-ICPMS),[9] atomic absorption spectrometry[10] and UV-Vis spectrophotometry,[11] as well as voltammetric techniques.[12,13] Voltammetry has been widely accepted for the detection of metals, such as Hg²⁺, because of its excellent sensitivity, straightforward procedure, low cost, and its suitability for *in situ* applications. However, particular aspects, such as a reasonable time scale of analysis, electrode modifications and selectivity need to be thoroughly assessed,[13] whereby straightforward and easy to implement electrode pre-treatment procedures have become desirable if not imperative. Electrode modifications using gold nanoparticles (AuNP) are commonly carried out for voltammetry.[14,15] AuNP are easy to synthesise, highly conductive, and increase the electrode surface area, making AuNPs an excellent choice in sensing applications. Employing AuNPs in combination with chemically selective capping agents, aggregation/agglomeration effects[16,17] can be minimised and selectivity of the modified electrode towards Hg²⁺ improved.

In this work, tannic acid ($C_{76}H_{52}O_{46}$, TA) is employed both as a stabilising agent for AuNPs and as a selective capping agent for Hg²⁺. TA is found in plant tissues, such as leaves, gallnuts, and pods of certain plants,[18] where it exhibits various structures, molecular masses, and physicochemical and biological properties.[19,20] In addition, TA molecules contains a large number of reactive functional groups, such as hydroxyl and phenolic hydroxyl groups, which can form complexes with heavy metal ions, such as Hg²⁺.[19,21] As an example, Luo *et al.*[22] have used TA modified Fe₃O₄ core–shell nanoparticles for the

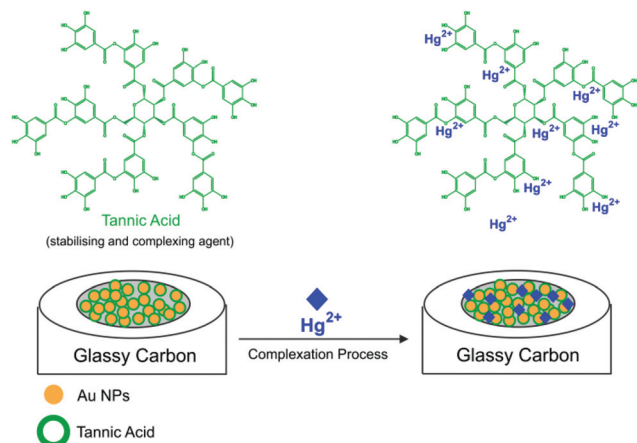*[a]Department of Chemistry, Physical and Theoretical Chemistry Laboratory, Oxford University, South Parks Road, Oxford OX1 3QZ, UK. E-mail: richard.compton@chem.ox.ac.uk; Fax: +44 (0)1865 275410; Tel: +44 (0)1865 275957*
[b]Department of Materials, Oxford University, Parks Road, OX1 3PH, UK
†Electronic supplementary information (ESI) available. See DOI: 10.1039/c8an00508g
‡Now at the school of Engineering and Applied Sciences, Harvard University, Cambridge, MA, USA.

Scheme 1 Tannic acid-capped gold nanoparticle modified glassy carbon electrode (AuNP@TA-GCE).

adsorption and detection of Hg^{2+} from contaminated water, and we have recently shown that the combination of AuNP and TA results in the sensitive detection of Al^{3+} in aqueous solutions with a "measurable lower limit" of 10.0 pM.[23] Furthermore, in biological related voltammetry applications, TA has been used as an electrode surface modifier for the detection of dopamine,[24] glucose,[25] bisphenol A[26] and epinephrine.[27] The role of TA appears to be either as a dopant,[24] as a biocompatible host for an enzyme[25] or the target,[26] or alternatively "electron mediation"[27] with TA is suggested. Despite apparent success in various applications, voltammetric strategies in connection with TA for the detection of inorganic Hg^{2+} have not been reported in literature.

In this work, we report the electrochemical detection of inorganic Hg^{2+} in aqueous solutions at a tannic acid-capped gold nanoparticle modified glassy carbon macroelectrode (AuNP@TA-GCE) by square wave voltammetry (SWV) (Scheme 1). The influence of coexisting ions on the detection of Hg^{2+} is investigated and Hg^{2+}-spiked tap water samples analysed. The developed sensing strategy is then transferred onto disposable AuNP@TA modified screen-printed electrodes (AuNP@TA-SPE), demonstrating the ability to detect Hg^{2+} in drinking water with a "measurable lower limit" of 100.0 fM, showing distinct signals above background, as well as making it accessible for routine monitoring applications.

Experimental

Chemicals

Mercury solutions were prepared from a 0.05 M mercury(II) nitrate ($Hg(NO_3)_2$, Sigma-Aldrich, Fluka Analytical, Steinheim, Germany) stock solution. For studies of interfering ions, zinc nitrate hexahydrate ($Zn(NO_3)_2$, >98%, Sigma-Aldrich, Steinheim, Germany) and aluminium sulphate ($Al_2(SO_4)_3 \cdot 16H_2O$, >97%, Alfa Aesar, Karlsruhe, Germany) were used as sources of Zn^{2+} and Al^{3+}. Tannic acid-capped gold

nanoparticles (AuNP@TA, 2.2×10^{10} particles per mL, NanoComposix, San Diego, USA), with a hydrodynamic diameter of 68.4 nm as indicated by the manufacturer, were used as received. Analyte solutions were prepared in a HCl–KCl solution (pH 1.0) by mixing 97.0 mL of 0.1 M HCl and 3.0 mL of 0.1 M KCl.[28] Nanopure water with a resistivity not less than 18.2 MΩ cm at 25 °C (Millipore water purification system, Millipak Express 20, Watford, UK), was used to prepare HCl and KCl solutions and to rinse electrodes during polishing. A high purity nitrogen flow (oxygen free, BOC Gases Plc) was used to degas analyte solutions prior to the electrochemical measurements.

Electrochemical apparatus

All electrochemical measurements were performed inside a Faraday cage (25 ± 1 °C) using a µAutolab Type III potentiostat (Metrohm u3AUT71335, Autolab B.V., Utrecht, The Netherlands). The potentiostat was interfaced to Windows PC with GPES software (version 4.9) for data acquisition. The utilised three electrode system consisted of a 1.48 ± 0.02 mm radius glassy carbon working electrode (CH Instruments, Inc., USA, GCE, size determined by optical microscopy), a saturated calomel reference electrode (SCE, Hg/Hg_2Cl_2, saturated KCl) and a 0.5 mm diameter platinum wire (Goodfellow Cambridge Ltd, UK), functioning as a counter electrode. Working electrodes were polished using a diamond spray of sizes 3, 1 and 0.1 micron (Kemet, Kent, UK) on soft microcloth polishing pads for approximately 3 minutes on each grade, rinsed in between with nanopure water. GCEs were modified by drop casting 25.8 µL of AuNP@TA suspension, which approximately corresponds to a surface concentration of one-monolayer (Calculation ESI 1†). The suspension was let to dry under nitrogen flow.

AuNP@TA characterisation

The size and aggregation/agglomeration characterisation of the AuNP@TA was carried out as described previously.[23]

Real sample analysis

The water sample used in this work was collected from the laboratory water tap. The collected tap water was spiked with various concentrations of Hg^{2+}. The influence of interfering metal ions was investigated using mixtures of tap water solutions containing Zn^{2+} and/or Al^{3+} at different concentrations.

The transfer of the established method to disposable screen-printed electrodes was realized using DropSens screen-printed carbon electrodes (DRP-110, DropSens, Llanera, Spain, SPEs), with a built-in carbon (4.0 mm diameter) working electrode, carbon counter electrode and silver reference electrode – all printed on a $L33 \times W10 \times H0.5$ mm ceramic substrate. SPEs were modified by drop casting 25.8 µL of AuNP@TA suspension and dried under N_2 flow. A 50.0 µL of sample solution was deposited onto the SPE surface, covering all three electrodes. Each sample was analysed in triplicate under optimised experimental conditions as discussed in the main text.

Results and discussion

In this section, we first discuss the electrochemical detection of inorganic mercury using cyclic voltammetry. The characterisation of AuNP@TA-GCEs in the absence and presence of Hg^{2+} at different scan rates, surface coverages and at various exposure times leads to the determination of a "measurable lower limit" for Hg^{2+}. The selectivity performance of the AuNP@TA-GCEs system towards possible interfering ions is discussed, before evaluating the detection of mercury using square wave voltammetry. As a proof of concept, we demonstrate the application of the established sensing strategy to screen-printed electrodes and real sample analysis.

Mercury detection by cyclic voltammetry

Optimization of CV parameters. The electrochemical characterisation of tannic acid (TA) in solution phase has been investigated previously, whereby an oxidation peak at a potential of 0.58 V *vs.* SCE was revealed.[23] Tannic acid capped gold nanoparticles (AuNP@TA) were characterized using scanning electron microscopy (Fig. S1†), showing a mean diameter size distribution of 60 ± 3 nm. Cyclic voltammetry of tannic acid capped gold nanoparticles-modified glassy carbon electrode (AuNP@TA-GCE) exposed to HCl–KCl (pH 1.0) results in an oxidation peak potential of TA at 0.31 V *vs.* SCE and describing a surface-controlled (adsorption) process.[23] In addition, prolonged exposure time of the AuNP@TA-GCE to the solution of HCl–KCl (pH 1.0), prior to CV measurements, revealed the swelling of the TA layers on the AuNP.[23]

Before assessing the oxidation behaviour of Hg^{2+} at AuNP@TA-GCEs, an unmodified glassy carbon electrode (GCE) was immersed in a solution of HCl–KCl (pH 1.0), containing 2.0 mM Hg^{2+} and CV was performed by sweeping the potential from 0.3 V to 0.7 V *vs.* SCE. No electrochemical current signal related to Hg^{2+} was observed (Fig. 1, black-solid curve), demonstrating the necessity for the proposed electrode modifications. To obtain fully functionalized AuNP@TA-GCEs sensors, AuNP@TA were drop casted onto a GCE surface at a concentration of about 5.7×10^8 nanoparticles, corresponding to a

surface concentration of approximately one-monolayer. The AuNP@TA-GCE was immersed in a solution of HCl–KCl (pH 1.0), containing 2.0 mM Hg^{2+}, whereby cyclic voltammograms (Fig. 1, red-solid curve) reveal two oxidation peaks at potentials of 0.40 V and 0.58 V *vs.* SCE, respectively. The first oxidation peak ("peak-1") is attributed to the oxidation of TA[23,29] and the second peak ("peak-2") is attributed to the AuNP@TA-Hg complex. Both peaks are increased as the capping agent layer swells and reflect the oxidation of phenolic or quinone groups in the TA.

The effect of scan rate was studied. A AuNP@TA-GCE was immersed into a 2.0 mM Hg^{2+} solution and CVs were recorded at scan rates of up to 0.12 V s^{-1}. As shown in Fig. S2a,† peak currents of both peak-1 and peak-2 increased monotonically with scan rate. The linear dependence of the peak currents of peak-1 and peak-2 on the scan rate (Fig. S2b†) suggests that both the oxidation process of TA and the AuNP@TA-Hg systems are surface-controlled (adsorption) processes. In addition, peak-1 substantially increases in the presence of Hg^{2+}, suggesting that the partial complexation of TA leads to a greater accessibility of the TA layers. The peak potential positions of peak-2 at 0.58 V *vs.* SCE were found to be independent of the scan rate, indicating a reversible electrochemical process for the oxidation of the AuNP@TA-Hg system. For further analytical measurements, a scan rate of 0.1 V s^{-1} was selected.

Next, the effect of the electrode surface coverage (surface concentration) of AuNP@TA on the Hg^{2+} uptake was studied. Coverages between 0.1 and 1.5-monolayers of AuNP@TA were evaluated, crudely estimating a close packing of 91% (Fig. S3a†).[30] All modified AuNP@TA-GCE with specific surface coverages were exposed to 2.0 mM Hg^{2+} in HCl–KCl (pH 1.0). As shown in Fig. S3b,† electrochemical peak currents of peak-1 and peak-2 enhanced monotonically with increasing AuNP@TA concentrations at the GCE surface. This is attributed to the greater number of accessible complexation sites of the AuNP@TA-GCE system. However, considering the cost of AuNP@TA, a surface coverage of one-monolayer was found to be sufficient for good analytical performance and thus was selected for further experiments.

One of the key aspects for achieving sufficient sensitivity and thus lowering the detection limit is the exposure time of the AuNP@TA-GCE system to Hg^{2+} ions in solution before voltammetric measurements. To evaluate this effect, a AuNP@TA-GCE was exposed to 1.0 μM Hg^{2+} in HCl–KCl (pH 1.0) at varying exposure times between zero to 30 minutes. As shown in Fig. 2, the peak current of peak-2 increased up to an exposure time of 10 min and significantly decreased at lengthier incubation. This effect can be attributed to the swelling of TA, which reaches its maximum at 10 min when the effective electrode surface becomes saturated with Hg^{2+}. This suggests that with a practical exposure time of 10 min good sensitivity of the AuNP@TA-GCE system towards the detection of Hg^{2+} by CV can be achieved.

"Measurable lower limit" for Hg^{2+} at AuNP@TA-GCE during CV. An exposure time of 10 min was applied to determine a

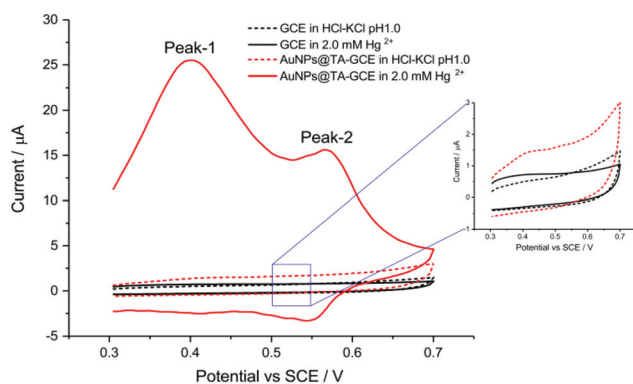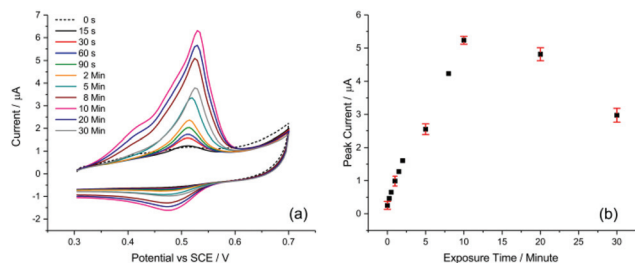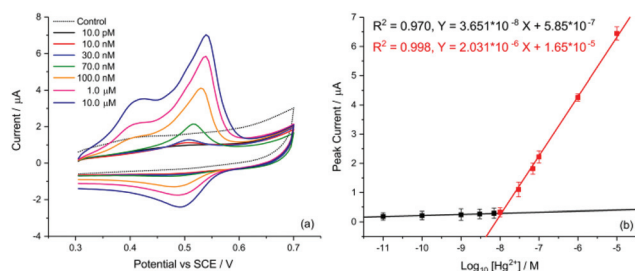**Fig. 1** Detection of Hg^{2+} at an unmodified GCE, as well as at a functionalized AuNP@TA-GCE at a scan rate of 0.1 V s^{-1}.

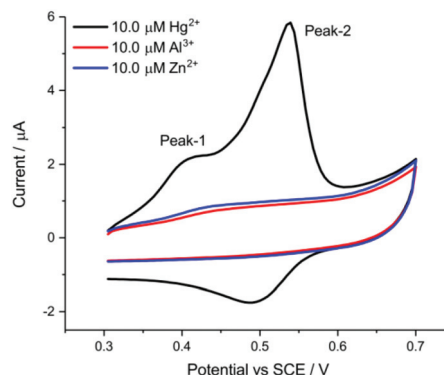**Fig. 2** Assessment of electrode exposure times to 1.0 μM Hg²⁺ by CV. (a) Voltammograms of AuNP@TA-GCE at various exposure times. (b) Current behaviour at peak-2 at exposures ranging from zero to 30 minutes.

Fig. 4 Selectivity performance of the AuNP@TA-GCE for Al³⁺ and Zn²⁺ at a scan rate of 0.1 V s⁻¹ and exposure time of 10 min.

"measurable lower limit", representing the lowest concentration that can be distinguished from the background signal, for the detection of Hg²⁺ by CV. As discussed in the section "Optimization of CV parameters", a surface coverage of one-monolayer of AuNP@TA and a scan rate of 0.1 V s⁻¹ were selected. The AuNP@TA-GCE was immersed in an HCl–KCl solution (pH 1.0) containing various Hg²⁺ concentrations, ranging from 10.0 pM to 10.0 μM (Fig. 3a). A linear base line correction was performed, which revealed two effective linear regions at concentrations of 10.0 pM–10.0 nM (Fig. 3b, black line) and 10.0 nM–10.0 μM (Fig. 3b, red line). These linear relationships indicate the potential for sensitive Hg²⁺ detection at low concentrations. Notably, a "measurable lower limit" was determined at 10.0 pM Hg²⁺, considerably lower than the guideline value of 30.0 nM for inorganic mercury in drinking water, as defined by the WHO.

Selectivity performance of the AuNP@TA-GCE system during CV. In order to develop an efficient sensor for the detection of mercury in the environment, possible interferences from other ions need to be excluded. As an example, a fully functionalized AuNP@TA-GCE was exposed to 10.0 μM Al³⁺ or Zn²⁺ and cyclic voltammetric measurements were performed applying the previously established optimal parameters. As shown in Fig. 4, a strong oxidation signal for Hg²⁺ was found without a significant contribution by neither Al³⁺, nor Zn²⁺ ions. We further note that TA is reported to forms a complex with Cu²⁺ but this is not electroactive.

We note that the start potential during the CV (and also for the SWV) sweeps being recorded plays a very important role to enable selectivity of sensing performance to Hg²⁺. A suitable start potential of 0.3 V vs. SCE allows the elimination of possible interference from Al³⁺.

The proposed Hg²⁺ detection strategy, based on AuNP@TA-GCE as described above, has shown the capability to selectively detect low concentrations of inorganic Hg²⁺ in aqueous solutions by CV. In the following, we discuss the possibility of avoiding exposure time as high as 10 min by conducting square wave voltammetry (SWV), which offers a reliable and more sensitive detection of Hg²⁺ for the routine monitoring and assessment of real samples.

Mercury detection by square wave voltammetry

Optimisation of SWV parameters. In order to reduce capacitive and background currents by SWV, several analytical parameters, such as exposure potential and time, frequency and pulse amplitude need to be optimized. To assess these parameters, the AuNP@TA-GCE system was exposed to 1.0 nM Hg²⁺ in HCl–KCl (pH 1.0). First, the effect of frequency on the current intensity was evaluated at a range from 10 to 50 Hz, while maintaining all other parameters constant (preliminary selection of amplitude of 0.03 V and an exposure time of 60 s). As shown in Fig. 5a, the peak current increased up to a value of 30 Hz and subsequently decreased at higher frequencies. Hence, 30 Hz was selected as the optimal frequency for Hg²⁺ detection. Second, the effect of amplitude variation on the AuNP@TA sensitivity was studied at different values, ranging from 0.01 to 0.05 V, while maintaining an optimal frequency of 30 Hz and a preliminarily selected exposure time of 60 s. As shown in Fig. 5b, the optimal amplitude of 0.04 V was found for Hg²⁺ detection, maximizing the electrochemical current signal. Finally, the exposure time was re-assessed for SWV in the range of zero to 90 s, while maintaining all other optimum parameters constant. The limiting value of peak current was obtained with an exposure time of 30 s (Fig. 5c). In summary, optimal parameters for the detection of Hg²⁺ using SWV selected to be at a frequency of 30 Hz, an amplitude of

Fig. 3 Detection of Hg²⁺ by CV. (a) Voltammograms of AuNP@TA-GCE at varying concentrations of Hg²⁺. (b) Linear peak current behaviour at various Hg²⁺ concentrations.
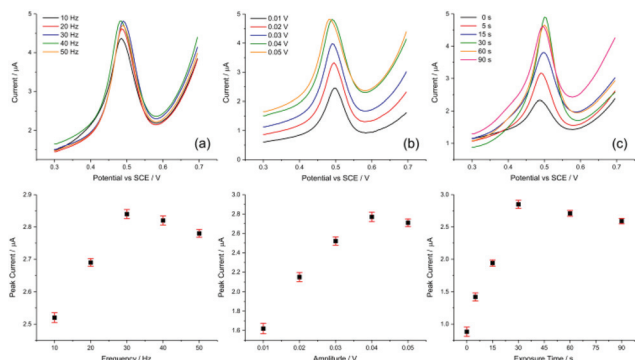
Fig. 5 Parameter optimisation for SWV. Evaluating (a) frequency, (b) amplitude, and (c) exposure time for the AuNP@TA-GCE system in HCl–KCl (pH 1.0), containing 1.0 nM Hg^{2+}.

0.04 V, and an exposure time of 30 s for all subsequent experiments.

Having defined the optimum conditions of SWV, the selectivity and sensitivity of the sensor is evaluated in the following section.

Selectivity performance of the AuNP@TA-GCE system during SWV. To assess the possible influence of various ions on the detection of Hg^{2+} at AuNP@TA-GCEs, solution mixtures of Hg^{2+}, Zn^{2+} and Al^{3+} in HCl–KCl (pH 1.0) in varying concentrations from 3.0 to 10.0 nM were prepared. As shown in Fig. S4,† both peak current and peak charge of the AuNP@TA-GCE system in the presence of possible interfering ions and Hg^{2+}, remained relatively constant (Table S1†). To obtain peak current values, a polynomial baseline correction (typically order 3) was performed and subtracted from the raw data. The resulting peak current and peak charge remains constant, indicating only minimal interference by these ions with the proposed Hg^{2+} sensor.

"Measurable lower limit" for Hg^{2+} at AuNP@TA-GCE during SWV. The sensitivity of the sensor was evaluated by immersing AuNP@TA-GCEs in HCl–KCl (pH 1.0), containing various Hg^{2+} concentrations, ranging from 100.0 fM to 100.0 nM (Fig. 6a). As described above, a polynomial baseline correction was conducted to determine peak current values (Fig. S5†). In the absence of Hg^{2+}, no peak current could be detected (Fig. 6a,

dotted line). As shown in Fig. 6b, a linear peak current behaviour was observed for peak-2 at concentrations ranging from 100.0 fM to 100.0 nM Hg^{2+}, revealing a "measurable lower limit", representing the lowest concentration that can be distinguished from the background signal, of 100.0 fM (Fig. 6a). Given the sensitivity of the proposed strategy, significantly below the permissible level of inorganic Hg^{2+} in drinking water of 30.0 nM,[1] and outperforming the system using CV, SWV compares favourably over other voltammetry approaches,[31–33] in addition to other methods, which require lengthier analysis time.[34,35]

Tap water analysis by AuNP@TA-GCE and SPCE/AuNP@TA using SWV. As a proof of concept, the characterized and optimized system for the detection of Hg^{2+} ions at AuNP@TA-GCE was exposed to Hg^{2+}-spiked tap water and SWV measurements were carried out. Tap water samples were collected in the laboratory and spiked with 20.0 µM, 2.0 µM and 20.0 nM Hg^{2+}. As shown in Fig. S6a,† the oxidation peak (oxidation of TA bound to Hg^{2+}) at a potential of roughly 0.60 V vs. SCE, increased with increasing Hg^{2+} concentrations in solution. Even a concentration of just 20.0 nM resulted in a significant peak current value in the presence of Hg^{2+}, in contrast to Al^{3+} and Zn^{2+} ions (Fig. S6b†). To validate the sensor's selectivity further, the AuNP@TA-GCE system was assessed in the presence of binary and ternary mixtures of tap water solutions, containing Zn^{2+} and/or Al^{3+} ions at a selected concentration of 20.0 nM for each ion. As shown in Fig. S6c,† the presence of Zn^{2+} and/or Al^{3+} in mixtures leads to an anodic peak current shift to a potential of roughly 0.67 V vs. SCE. The conducted polynomial baseline correction revealed, both peak current and peak charge of the binary and ternary solutions remained relatively constant to the value in the presence of 20.0 nM Hg^{2+}-spiked tap water. These results demonstrate that the AuNP@TA-GC sensor retains its selectivity towards Hg^{2+}, even if applied to more complex media, such as tap water.

Finally, the transfer of this strategy onto disposable screen-printed electrodes (SPEs) may facilitate the utilization of the demonstrated analytical method in portable devices for routine monitoring. Bare carbon SPEs were modified by drop casting AuNP@TA at an approximate surface concentration of one-monolayer (assuming the particles are uniformly dispersed on the SPE surface). Cyclic voltammetry was conducted to assess whether the oxidation of the AuNP@TA system in the absence of Hg^{2+} is a surface-controlled or diffusion-controlled process. The modified AuNP@TA-SPE was immersed into HCl–KCl (pH 1.0) and CV measurements were carried out at scan rates from 10 to 125 mV s^{-1}. As shown in Fig. S7b,† a linear dependence of the peak current on the scan rate was observed, suggesting a surface-controlled process. Furthermore, the peak potential positions at roughly 0.04 V vs. Ag were found to be independent of the scan rate, indicating an electrochemically reversible process. To detect Hg^{2+} at AuNP@TA-SPEs and to establish a calibration curve, functionalized sensors were immersed in HCl–KCl (pH 1.0), containing various Hg^{2+} concentrations ranging from 10.0 pM to 1.0 µM (Fig. 7a). As shown in Fig. 7b, a linear dependence of the peak current as a

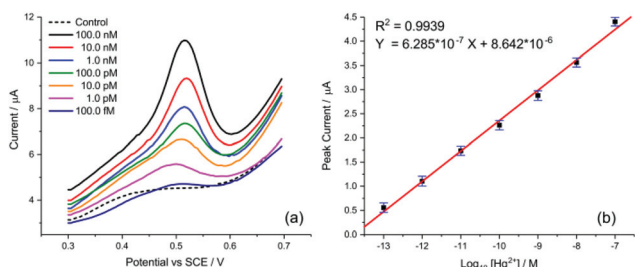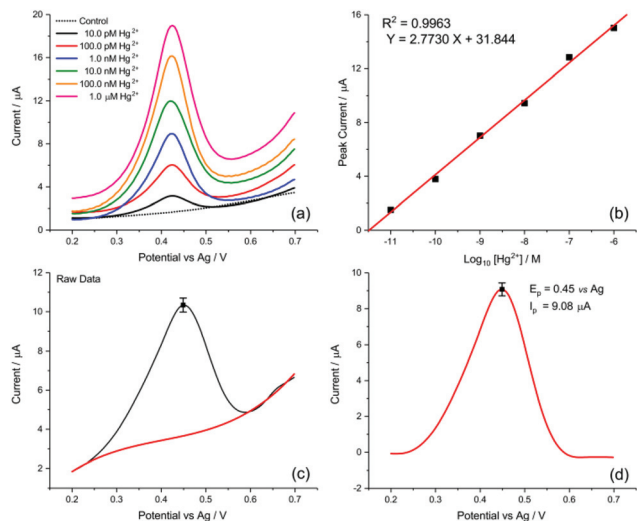

Fig. 6 Detection of Hg^{2+} by SWV. (a) Voltammograms of AuNP@TA-GCE at varying concentrations of Hg^{2+}. (b) Linear peak current behaviour. Error bars represent relative standard deviation.

Fig. 7 Detection of Hg^{2+} by SWV using AuNP@TA-SPEs. (a) Voltammograms of AuNP@TA-SPEs exposed to various Hg^{2+} concentrations in HCl–KCl. (b) Linear peak current behaviour for various Hg^{2+} concentrations. (c) Detection of 10.0 nM Hg^{2+} in tap water. Raw data (black curve) with polynomial baseline (red curve). (d) Resulting curve after subtraction of polynomial baseline from raw data. Note that error bars represent the relative standard deviation from triplicate experiments.

function of $\log_{10}$ of Hg^{2+} concentrations was observed, whereby a relative standard error of 26% for the determination of Hg^{2+} concentration from the calibration curve was calculated (see ESI† for details). This error value highlights the excellent sensitivity of the proposed sensing principle, as concentrations of roughly one order of magnitude below the critical limit of 30.0 nM, defined by the WHO, can be distinguished with statistical significance. Therefore, the relationship of the peak current as a function of $\log_{10}$ of Hg^{2+} concentrations can further be used to determine possible Hg^{2+} contamination in tap water.

The detection of inorganic Hg^{2+} in tap water using AuNP@TA-SPEs was conducted by exposing the sensor to tap water, spiked with 10.0 nM Hg^{2+}. SWV was performed in triplicates and experimental parameters were selected in accordance with optimisation procedures outlined above. As shown in Fig. 7c, a clear electrochemical oxidation peak current can be seen at a potential of 0.45 V vs. Ag, with an average peak current value of 9.08 ± 0.17 µA. According to the linear calibration function (Fig. 7b), this current value corresponds to an Hg^{2+} concentration in solution with an average of 9.27 nM, close to the theoretical value of 10.0 nM, showing a recovery above 90%.

Conclusions

The presented work demonstrates an effective analytical method for the sensitive and selective electrochemical detection of inorganic Hg^{2+} in aqueous solutions, based on tannic

acid capped gold nanoparticles at carbon electrodes. This strategy allows the quantitative analysis of Hg^{2+} in real samples, such as tap water. We have characterized the electrochemical sensing parameters for cyclic voltammetry and square wave voltammetry and excluded signal contributions from possibly interfering Al^{3+} and Zn^{2+} ions. This strategy for the detection of trace and/or ultra-trace levels of inorganic Hg^{2+} in aqueous solutions exhibits a "measurable lower limit" of 100.0 fM. The transfer of the analytical method onto screen-printed electrodes makes it suitable for the routine monitoring of inorganic Hg^{2+} in drinking water, as it meets the critical threshold value of 30.0 nM, set by the WHO.

Conflicts of interest

There are no conflicts to declare.

Acknowledgements

References

1 WHO, *Guidelines for drinking-water quality: Fourth edition incorporating the first addendum*, 2017.
2 Y. Li, B. He, L. Hu, X. Huang, Z. Yun, R. Liu, Q. Zhou and G. Jiang, *Talanta*, 2018, **178**, 811–817.
3 P. Chakraborty, *Sci. Total Environ.*, 2017, **589**, 232–235.
4 A. T. Khan, A. Atkinson, T. C. Graham, S. J. Thompson, S. Ali and K. F. Shireen, *Toxicology*, 2004, **42**, 571–577.
5 G. Bjørklund, M. Dadar, J. Mutter and J. Aaseth, *Environ. Res.*, 2017, **159**, 545–554.
6 Y. Liu, S. McDermott, A. Lawson and C. Marjorie Aelion, *Int. J. Hyg. Environ. Health*, 2010, **213**, 116–123.
7 D. Peplow and S. Augustine, *Environ. Sci.: Processes Impacts*, 2014, **16**, 2415–2422.
8 K. M. Rice, E. M. Walker, M. Wu, C. Gillette and E. R. Blough, *J. Prev. Med. Public Health*, 2014, **47**, 74–83.
9 J. Hu, E. Pagliano, X. Hou, C. Zheng, L. Yang and Z. Mester, *J. Anal. At. Spectrom.*, 2017, **32**, 447–2454.
10 M. Senila, E. Covaci, O. Cadar, M. Ponta, M. Frentiu and T. Frentiu, *Chem. Pap.*, 2018, **72**, 441–448.
11 E. Ghasemi and M. Kaykhaii, *Eurasian J. Anal. Chem.*, 2017, **12**(4), 313–324.
12 D. Martín-Yerga and A. Costa-García, *Curr. Opin. Electrochem.*, 2017, **3**, 91–96.

13 A. L. Suherman, E. E. L. Tanner and R. G. Compton, *TrAC, Trends Anal. Chem.*, 2017, **94**, 161–172.

14 K. Saha, S. S. Agasti, C. Kim, X. Li and V. M. Rotello, *Chem. Rev.*, 2012, **112**, 2739–2779.

15 S. Zeng, K.-T. Yong, I. Roy, X.-Q. Dinh, X. Yu and F. Luan, *Plasmonics*, 2011, **6**, 491–506.

16 K. Ngamchuea, K. Tschulik, S. Eloul and R. G. Compton, *ChemPhysChem*, 2015, **16**, 2338–2347.

17 S. V. Sokolov, K. Tschulik, C. Batchelor-McAuley, K. Jurkschat and R. G. Compton, *Anal. Chem.*, 2015, **87**, 10033–10039.

18 J. Wang, C. Zheng, S. Ding, H. Ma and Y. Ji, *Desalination*, 2011, **273**, 285–291.

19 M. A. Rahim, H. Ejima, K. L. Cho, K. Kempe, M. Müllner, J. P. Best and F. Caruso, *Chem. Mater.*, 2014, **26**, 1645–1653.

20 B. H. Cruz, J. M. Díaz-Cruz, C. Ariño and M. Esteban, *Electroanalysis*, 2000, **12**, 1130–1137.

21 L. Fan, Y. Ma, Y. Su, R. Zhang, Y. Liu, Q. Zhang and Z. Jiang, *RSC Adv.*, 2015, **5**, 107777–107784.

22 H. Luo, S. Zhang, X. Li, X. Liu, Q. Xu, J. Liu and Z. Wang, *J. Taiwan Inst. Chem. Eng.*, 2017, **72**, 163–170.

23 A. L. Suherman, E. E. L. Tanner, S. Kuss, S. V. Sokolov, J. Holter, N. P. Young and R. G. Compton, *Sens. Actuators, B*, 2018, **265**, 682–690.

24 L. Jiang, Q. Xie, Z. Li, Y. Li and S. Yao, *Sensors*, 2005, **5**, 199–208.

25 B. Çakiroğlu and M. Özacar, *Electroanalysis*, 2017, **29**, 1–9.

26 K. Rajar, R. A. Soomro, Z. H. Ibupoto, Sirajuddin and A. Balouch, *Int. J. Food Prop.*, 2017, **20**, 1359–1367.

27 J. G. Manjunatha, B. E. Kumara Swamy, G. P. Mamatha, O. Gilbert, B. N. Chandrashekar and B. S. Sherigara, *Int. J. Electrochem. Sci.*, 2010, **5**, 1236–1245.

28 C. Mohan, A guide for the preparation and use of buffers in biological systems, *Calbiochem*, 2003, 18–21.

29 D. L. Vu, B. Ertek, Y. Dılgın and L. Červenka, *Czech J. Food Sci.*, 2015, **33**, 72–76.

30 E. Kätelhön, W. Cheng, C. Batchelor-McAuley, K. Tschulik and R. G. Compton, *ChemElectroChem*, 2014, **1**, 1057–1062.

31 A. Shah, S. Sultan, A. Zahid, S. Aftab, J. Nisar, S. Nayab, R. Qureshi, G. S. Khan, H. Hussain and S. A. Ozkan, *Electrochim. Acta*, 2017, **258**, 1397–1403.

32 E. Granado, E. Gervais, G. Gotti, S. Desclaux, M. Meireles, P. Gros and D. Evrard, *Int. J. Electrochem. Sci.*, 2017, **12**, 6092–6107.

33 H. L. Nguyen, H. H. Cao, D. T. Nguyen and V.-A. Nguyen, *Electroanalysis*, 2017, **29**, 595–601.

34 K. Asadpour-Zeynali and R. Amini, *Sens. Actuators, B*, 2017, **246**, 961–968.

35 M. P. N. Bui, J. Brockgreitens, S. Ahmed and A. Abbas, *Biosens. Bioelectron.*, 2016, **85**, 280–286.